



Energy efficiency of latent heat storage systems in residential buildings: Coupled effects of wall assembly and climatic conditions

J. Kočí^{*}, J. Fort, R. Černý

Department of Materials Engineering and Chemistry, Faculty of Civil Engineering, Czech Technical University in Prague, Thákurova 7, Prague 6, 166 29, Czech Republic



ARTICLE INFO

Keywords:

Phase change material
Energy savings
Building
Plaster
Energy consumption
Computational modeling
Climatic load
Wall assembly

ABSTRACT

The European Union emphasizes the decrease in energy consumption of buildings as a key priority of its energy policy. Incorporation of phase change materials (PCMs) into conventional building materials is considered as a solution which may partially contribute to the efforts aimed at meeting this priority. Although promising results have been achieved, some PCM-utilization related issues are still to be addressed in order to fill the gaps in the field of real-world applications. In this paper, the effect of plasters modified by PCM on diatomite- and *n*-dodecanol basis on the energy performance of building envelopes is analyzed, taking into account various climatic loads and material compositions characteristic for the European countries. The obtained results, which are based on coupling the geographical and structural aspects, provide a good background for the assessment of suitability of PCM applications in building envelopes. The efficiency of the analyzed latent heat storage systems is found very sensitive to a combination of material composition and geographical locations. In precisely tailored applications, possible annual savings on heating and cooling can range between 3.7 and 6.5 kWh per square meter of the façade. However, most of the PCM-based systems should be considered with caution as both economic and environmental feasibility is not unambiguous. As the present state of the art focuses mainly on specific load bearing structures or locations, the conceptual approach presented in this study can bring a new insight into the utilization of latent heat storage systems in residential buildings.

1. Introduction

Energy consumption poses one of the major concerns for present society due to increased prices as well as for increasing awareness since energy production based on fossil fuel combustion harms the global climate. On this account, energy efficiency became one of the widely spoken terms across various sectors. Considering a rapid development in the global population and urbanization, the buildings became the most energy-intensive sector in the world which is responsible for over 40% of global energy consumption and it should grow up to 50% by 2050 as reported by Ref. [1]. According to the datasheet presented in the aforementioned report, the proportional distribution of energy allocated for residential buildings is plotted in Fig. 1. Here, a dominant share is expended for space heating and cooling of building interiors in order to maintain an ideal ambient climate [2–4]. Concurrently with efforts aimed at a decrease in energy consumption expended for space heating and cooling, the requirements paid on thermal comfort for buildings inhabitants need to be secured for the preservation of health [3,5–8].

One of the promising strategies extensively studied by many

researchers can be found in the employment of thermal energy storage systems based on the utilization of phase change materials that absorb and release energy during melting and solidification [9–14]. The whole latent heat storage concept consists in mitigation of diurnal peak temperatures, thus passive cooling/heating of building interiors and consequent energy savings thanks to the preservation of desired indoor climate conditions [14–16]. Application of PCM in the building sector became highly studied and discussed topic during last several decades. In this sense, a number of studies have been carried out with various attitudes and scientific approaches to this topic [17]. Researchers often focused on the development of new PCMs [18–20], their material characterization [21–23], or incorporation of various types of PCMs into conventional building materials [9,24–28]. The performance analysis of integrated PCMs was also of a high interest, aimed at the quantification of their benefits or optimization of their efficiency. Here, the major part presented various parametric studies and analyses covering the effect of building envelope design [30,31], wall type and orientation [32–35], climatic conditions [36–50], heating and cooling systems [51–54], or building operations [53,55] on the efficiency of latent heat storage systems. Many of those studies were devoted to real-time in-situ

* Corresponding author.

E-mail address: jan.koci@fsv.cvut.cz (J. Kočí).

List of symbols

Latin symbols

a	thermal diffusivity ($\text{m}^2 \cdot \text{s}^{-1}$)
c	specific heat capacity ($\text{J} \cdot \text{kg}^{-1} \cdot \text{K}^{-1}$)
A	water absorption coefficient ($\text{kg} \cdot \text{m}^{-2} \cdot \text{s}^{-1/2}$)
ΔH	phase change enthalpy ($\text{J} \cdot \text{g}^{-1}$)
H	enthalpy density ($\text{J} \cdot \text{m}^{-3}$)
L_v	latent heat of evaporation of water ($\text{J} \cdot \text{kg}^{-1}$)
M	molar mass of water vapor ($\text{kg} \cdot \text{mol}^{-1}$)
p_v	partial pressure of water vapor in the porous space (Pa)
R	universal gas constant ($\text{J} \cdot \text{K}^{-1} \cdot \text{mol}^{-1}$)
R_c	compressive strength (MPa)
R_f	flexural strength (MPa)
T	absolute temperature (K)
ΔT_e	temperature difference between the opposite sides of the element in the main direction of the heat flux (K)

T_m	melting onset temperature ($^\circ \text{C}$)
T_s	solidifying onset temperature ($^\circ \text{C}$)
W	moisture content by volume ($\text{m}^3 \cdot \text{m}^{-3}$)
Δx_e	thickness of the element in the main direction of the heat flux (m)

Greek symbols

δ_p	water vapor diffusion permeability (s)
κ	moisture diffusivity ($\text{m}^2 \cdot \text{s}^{-1}$)
λ	thermal conductivity ($\text{W m}^{-1} \text{K}^{-1}$)
$\lambda_p(w,t)$	moisture-dependent thermal conductivity of the interior plaster element ($\text{W m}^{-1} \text{K}^{-1}$)
μ	water vapor diffusion resistance factor (-)
ρ	matrix density ($\text{kg} \cdot \text{m}^{-3}$)
ρ_v	bulk density ($\text{kg} \cdot \text{m}^{-3}$)
ρ_w	density of water ($\text{kg} \cdot \text{m}^{-3}$)
ψ	total open porosity (-)

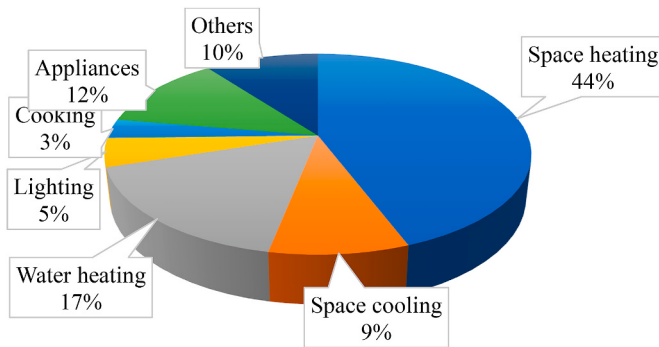


Fig. 1. World building final energy consumption by end-use in 2018.

monitoring of incorporated PCM into building materials [21,56,57].

In general, the vast majority of published papers exalted the utilization of PCMs in the building sector, acknowledging their beneficial effects such as heating and cooling energy savings, stabilization of indoor temperature and enhancing thermal comfort, or mitigation of overheating risks. However, the interpretation of results obtained from experimental or numerical studies did not always match with a proper understanding of the phase change phenomenon in building envelopes, which could lead to overestimation of the effect of PCMs or claiming credit for something that those materials do not deserve. An understanding of the phase change phenomenon in relation to utilization of the latent heat for a passive cooling/heating of buildings poses a crucial parameter for the viability of such an approach [58,59]. For example, the definition of phase change temperature as a single value, as assumed by Aketouane et al. [60], is not sufficient for description of the real performance of PCMs since the phase change transition represents a more complex phenomenon that requires experimental verification. Seeing that subcooling is very common during the phase change between solid and liquid phase, the employment of only one temperature-dependent enthalpy curve may result in substantial misrepresentation and diminished material performance in real application [11,51] due to neglect of hysteresis, as concluded by Mehling et al. [61] or Barz and Sommer [62].

The principal condition for the real efficiency of PCMs lays in surpassing phase change temperature on a daily basis, in the ideal case. However, several studies completely omitted this requirement and concluded that the observed benefits were achieved by latent heat storage without performing phase change transition due to limited

diurnal temperature fluctuation [63]. Such benefits could though be rather attributed to the lower thermal conductivity of the new PCM containing layer [64].

To evaluate the energy saving potential of PCMs in real applications, it is very important to understand properly the physical principles of phase change transition that occur in building materials. However, the entire application should be perceived in the context of local conditions and environment as well. As concluded by Park et al. [65], the PCM application needs to be tailored for particular climatic conditions to achieve maximal total annual energy savings due to sensitivity to phase change temperature. Most of the studies devoted to energy efficiency of PCMs are focused on particular location or climatic zone only, indeed. For example, thermal performance or energy saving potential of buildings with integrated PCM was studied in hot arid climate [46,66,67], tropical climate [47,48,52], subarctic climate [49], continental climate [50], etc. Several authors focused on particular country, such us Japan [37], Australia [38], Latvia [68], Spain [39], Morocco [40,41], India [42], United Arab Emirates [43], Iran [44], or South Korea [45]. Those studies provided valuable data and scientific findings. However, the multi-climate aspect was missing, i.e. it was very difficult to deduce how the PCM from one region will respond if applied in another one. Although some studies dealt with this issue [69,70], only one type of load-bearing construction was usually dealt with, often classified as light- or heavy-weight construction. Such an approach did not though provide a multi-structural insight on the suitability of a PCM application.

Since the European Union emphasizes a substantial reduction of energy consumption of buildings, the energy saving potential of latent heat storage systems represents an important task that needs to be properly described. The present state-of-the-art does not provide a robust and comprehensive evaluation of the PCM effectiveness including the effect of major variables and remains focused mainly on specific load-bearing structures or locations. Therefore, the conceptual approach presented in this study should bring a new insight into the assessment of PCM utilization in residential buildings, which is based on the relationship between the composition of the building envelope and the climatic conditions in the European region. In a practical demonstration of the proposed methodology, the possible energy savings of PCM-modified interior plasters are investigated under 64 different scenarios covering various load-bearing structures, climatic zones, and plaster modifications. The in-depth analysis of each scenario provides important data that are crucial to understand the energy performance of PCM plasters in various conditions. Based on the obtained results, the main findings are summarized, providing basic guidelines for a tailored design and application of advanced PCM envelope systems in residential

buildings across Europe.

2. Studied materials

The shape-stabilized PCM (SS-PCM) was prepared by vacuum saturation using the highly porous diatomite powder as the skeleton support material (LB Minerals, Czech Republic) and *n*-dodecanol (Sigma-Aldrich, Germany) having the temperature of phase change of the pure *n*-dodecanol of 22 °C and the latent heat of 170 J g⁻¹ [71]. Within this study, the diatomite/dodecanol ratio of about 1/0.85 was chosen based on the preliminary research. The synergic effect of the pozzolanic activity of diatomite and increased thermal storage capacity of such composite predetermined material suitability for utilization in building materials. The formed PCM composite (SS-PCM) revealed the phase change temperature of 23.15 °C for the cooling cycle, and 21.13 °C for heating respectively. The specific enthalpy was 71.36 J g⁻¹ during cooling and 73.1 J g⁻¹ during the heating cycle [71].

Consequently, the plasters modified by PCM were designed using the commercial dry cement-lime plaster mixture Manu 1 (Baumit, Germany) as the reference material. The modified mixtures were designed by adding SS-PCM admixture of about 8, 16, and 24 wt% (denoted as P8, P16, and P24). Mechanical, thermal and hygric properties of designed SS-PCM plaster are given in Table 1.

3. Computational analysis

The computational analysis was aimed at investigation of the effect of studied advanced plasters on the energy performance of the building envelopes exposed to various climatic loads typical for Europe. The emphasis was put on identification of energy improvements that may potentially result from those applications. The experimental data determined in laboratory conditions were used as input parameters and two-scale modeling approach was adopted to investigate the building envelopes and indoor environment exposed to the dynamic exterior conditions. In total, four different wall assemblies and four different interior plasters were studied. All the combinations were subjected to environmental loads defined by four different climate zones in Europe generating 64 different scenarios for simulations. The investigation should reveal the most suitable scenario of SS-PCM plasters application and demonstrate how the climate can affect the overall performance of SS-PCM plasters by the identification of the correlations between material composition of the wall and location. Fig. 2 shows the flowchart depicting the applied methodology. The main advantage of the proposed methodology consists in the fact that it can be easily extended to any other wall type, material and geographical location. Additionally, the parameters of building envelope can be simply adjusted to cover practically any building design used in Europe. This allows the methodology to be applied not only for residential, but also commercial and industrial building sector.

Table 1

Mechanical, thermal and hygric properties of designed SS-PCM plasters.

	Parameter/mixture	RP	P8	P16	P24
Physical properties	ρ_v (kg m ⁻³)	1572	1448	1386	1321
	ρ (kg m ⁻³)	2415	2294	2179	1982
	ψ (%)	34.9	37.8	35.3	35.6
	R_c (MPa)	1.91	1.8	1.73	1.69
Thermal properties	R_f (MPa)	0.9	0.83	0.78	0.73
	λ (W m ⁻¹ K ⁻¹)	0.54	0.52	0.53	0.53
	a (m ² s ⁻¹)	0.36	0.33	0.34	0.34
	ΔH (J g ⁻¹)	–	4.63	10.11	15.2
Hygric properties	T_m (°C)	–	22.46	22.13	22.68
	T_s (°C)	–	20.68	22.81	22.75
	κ (m ² s ⁻¹)	5.66·10 ⁻⁷	5.87·10 ⁻⁷	6.23·10 ⁻⁷	6.80·10 ⁻⁷
	A (kg m ⁻² s ^{-1/2})	0.203	0.231	0.215	0.209
	μ (–)	9.4	8.9	8.5	8.3

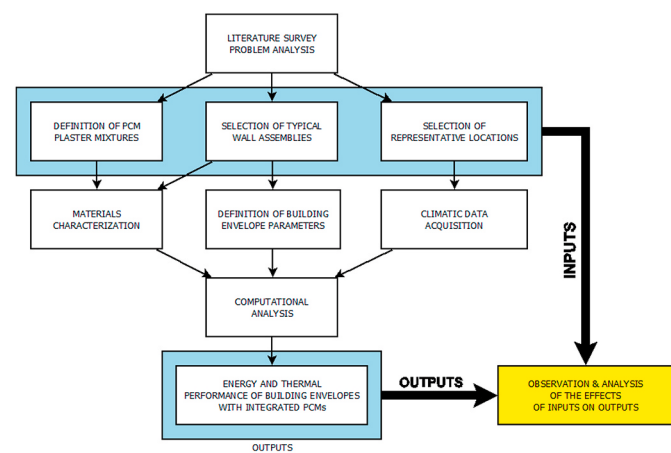


Fig. 2. Flowchart of applied methodology.

3.1. Case study

Within the computational analysis, the particularly studied plasters were applied in a thickness of 20 mm on the interior surface of the structural wall built from two typical load-bearing materials – autoclaved aerated concrete (AAC) with the thickness of 500 mm, and ceramic brick with the thickness of 450 mm. In the next step, both structural walls were provided by 100 mm layer of mineral wool on the exterior surface to include the effect of reduced heat transfer on SS-PCM plaster behavior. Since the material parameters of both AAC, ceramic brick and thermal insulation were not measured within the presented work, they were adopted from previous research and accessed in Table 2 [72]. The following *U*-values were calculated for each wall assembly: uninsulated ceramic brick wall – 0.993 W m⁻² K⁻¹, insulated ceramic brick wall – 0.264 W m⁻² K⁻¹, uninsulated AAC wall – 0.137 W m⁻² K⁻¹, and insulated AAC wall – 0.099 W m⁻² K⁻¹.

In the case study, the south-oriented room was simulated with the different exterior walls provided with SS-PCM plasters. The effect of interior plasters was studied using indoor air temperature analysis. The studied room was 5-m-wide and the heat balance governing the room

Table 2
Basic physical, thermal and hygric properties of applied materials.

Material parameter	Ceramic brick	AAC P1.8-300	Mineral wool
ρ_v (kg m ⁻³)	1831	289	70
ρ (kg m ⁻³)	2581	2206	2260
ψ (%)	27.9	86.9	96.9
λ (W m ⁻¹ K ⁻¹)	0.59	0.071	0.036
c (J kg ⁻¹ K ⁻¹)	825	1090	810
μ (–)	22.1	15.61	2.62

temperature variations during the reference year included heat transfer through the exterior wall, effect of solar heat gains through glazing and air infiltration. The scheme of the studied room is shown in Fig. 3. More details on the computational model are provided in the following subsections.

3.2. Computational model

The effect of SS-PCM plasters in the composition of multilayered building walls was studied by two-scale modeling using two interconnected models. The heat and moisture transport through the wall assembly was modelled by a modified version of Künzel's model [73] with the following balance equations:

$$\frac{dH}{dT} \frac{\partial T}{\partial t} = \text{div}(\lambda \text{grad}T) + L_v \text{div}(\delta_p \text{grad}p_v), \quad (1)$$

$$\left[\rho_w \frac{dw}{dp_v} + (\psi - w) \frac{M}{RT} \right] \frac{\partial p_v}{\partial t} = \text{div}[D_g \text{grad}p_v], \quad (2)$$

For more details on modification of the original Künzel's model including the motivation for such modification please refer to Madera et al. [74]. The phase change in this model was described by the fixed-domain method, which is very efficient and easy-to-use approach [75]. Within this approach, specific enthalpy as function of temperature determined using DSC device can be easily implemented. Slope of such function represents an effective specific heat capacity that can be implemented in the heat balance equation. All the simulations of the heat and moisture transport in the building envelope were done by finite element method (FEM) using general solver SIFEL (SImple Finite Elements) [76]. The pre-processing including mesh generation was done by HMS tool. Validation of such a solution for solving engineering tasks combining both HMS and SIFEL package has been done in the recent past [77].

The hygrothermal simulations performed according to Eqs. (1) and (2) allowed for the determination of the hourly values of the surface heat flux densities that were used as one of the input parameters required by the indoor air model. The heat flux density was calculated as

$$q(t) = \lambda_p(w, t) \frac{\Delta T_c(t)}{\Delta x_e} \quad (3)$$

The one-dimensional simulation of heat and moisture through the wall assembly was complemented by the one-dimensional indoor temperature model that was interconnected with the Künzel's mathematical model and exchanged data with that model during the simulation. The indoor temperature model was based on steady-state calculation of interior thermal mass in each time step. The interior thermal mass consisted of an indoor air layer and a partition wall, where each layer was defined by volumetric heat capacity multiplied by layer thickness.

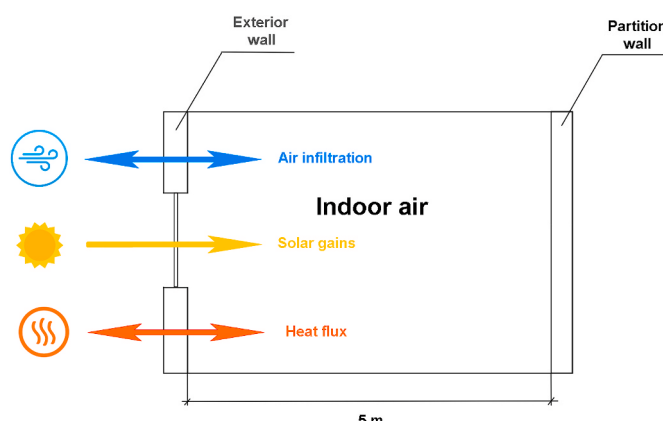


Fig. 3. Scheme of studied room.

Thus, the model was able to calculate the steady-state temperature of the interior thermal mass from the heat flux density provided by Künzel's model, solar gains through transparent building elements (windows) and the effect of air infiltration. The scheme of computational modeling is shown in Fig. 4. The solar gains were calculated from direct and diffuse solar radiation for each location, solar heat gain coefficient of the window (SGHC) and glazing percentage of the façade, i.e. the ratio between transparent and total façade surface. The heat losses or gains from air infiltration were calculated using the differences between interior and exterior air temperature and air exchange rate. The model can be simply extended by adding heat generation terms simulating building occupancy or operation of appliances and machines, as well as other aspects like natural ventilation, etc. However, in this case, the solar heat gains, air infiltration and heat flux through building envelopes was believed to be sufficient for sake of comparison of the effect of different SS-PCM plaster applications.

In light of this, the Künzel's model associated with the indoor temperature model allowed for simulation of temperature variations that can be further analyzed. More to that, if temperature variation during a year is known, heating and cooling energy demands can be easily calculated by defining heating and cooling setpoints. If the temperature drops below the particular user-defined setpoint, the energy necessary for heating-up the interior to the desired temperature level can be accounted for as a heating energy demand. Similarly, if the indoor temperature exceeds a user-defined threshold, the energy removed from the interior is accounted as cooling energy demand. The heating and cooling setpoints in this particular research were set identically for all wall types regardless of the location to allow direct comparison between individual scenarios and reveal potential benefits and drawbacks of SS-PCM plaster applications. Studied building walls and indoor space were oriented to the south in order to maximize the effect of SS-PCM plasters on energy performance and thermal comfort. The model parameters used in the computational simulations are listed in Table 3.

3.3. Boundary conditions

In this study, four locations in Europe were chosen. According the often used Koppen and Geiger climate classification [78], the climate is classified into five main climate groups, with each group being divided based on seasonal precipitation and temperature patterns. In this research, the dry climate (class B), the temperate climate (class C) and continental climate (class D) were studied as a typical representative for the major part of Europe. Within these classes, Prague (Czech Republic), Porto (Portugal), Sevilla and Valencia (Spain) were selected to cover four different temperatures and precipitation loads. Prague is typical with warm-summer humid continental climate (Dfb classification), Porto with a warm-summer Mediterranean climate (Csb), Sevilla with cold semi-arid climate (Bsk), and finally Valencia with a hot-summer Mediterranean climate (Csa). The weather data for each location was obtained using Meteonorm software in the form of the Test Reference Year (TRY). TRY contains artificial annual climate derived from weather observations and measurements at a certain location over past several decades. For the illustration, the average monthly temperatures and relative humidities are shown in Fig. 5. However, in the simulations, the complete dynamic hourly data provided from TRY were adopted that included also precipitation, solar radiation, wind speed and direction to describe the exterior boundary conditions.

The average monthly temperatures indicate significant differences between individual locations that will affect the thermal performance of studied building envelopes including the response of PCM plasters. This should be definitely taken into consideration when performance analysis is conducted. The following annual average temperatures were calculated for the studied locations: Prague 10.13 °C, Porto 14.87 °C, Sevilla 18.22 °C, and Valencia 17.66 °C.

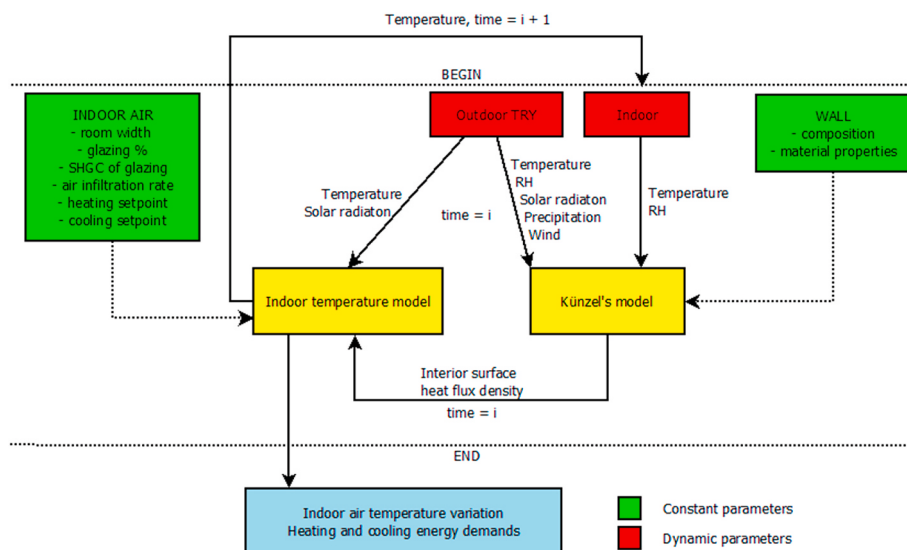
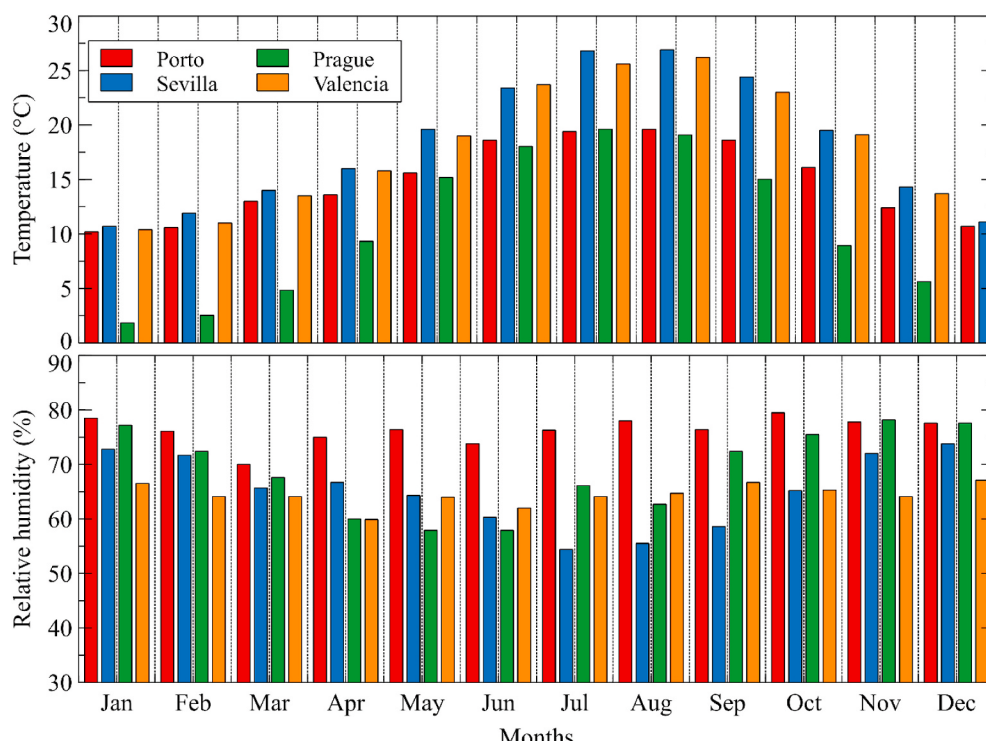
**Fig. 4.** Flowchart of computational modeling.

Table 3
Indoor temperature model parameters.

Parameter	Value
Room width (m)	5.0
Interior heat capacity per 1 m ² of the wall (J m ⁻² K ⁻¹)	2.6·10 ⁵
Solar radiation (W m ⁻²)	Hourly data from TRY
Glazing percentage (-)	0.3
SHGC of the windows (-)	0.6
Air infiltration rate (h ⁻¹)	0.6
Heating setpoint (° C)	20.0
Cooling setpoint (° C)	24.0

4. Results

In this section, the results of the computational analysis are presented. The two-scale model provided a wide range of hourly data describing the hygrothermal performance of the wall assembly, daily fluctuations of interior temperature and space heating and cooling energy demands for each studied scenario. Concerning environmental policy and the effort to reduce energy consumptions in the building sector, space heating and cooling energy demands were analyzed as the most important outputs of this research. The heating and cooling energy consumptions were calculated per unit area of the façade wall adjacent to the investigated room with defined parameters to estimate the potential benefits induced by the SS-PCMs in the plaster mixtures. The selected range of material compositions and climatic loads with different

**Fig. 5.** Monthly averaged temperature and relative humidity from TRY for studied locations.

severities and environmental effects provided sufficient diversity allowing investigation of SS-PCM plaster applications and their responses under various conditions. In every studied scenario, the best results were achieved for P24 plaster that contained the highest amount of SS-PCM among the analyzed plaster mixtures. Therefore, the results and comments provided in the following subsections are associated with P24 plasters only and compared to the reference plasters to demonstrate the improvement in the energy performance of the wall assembly.

4.1. Ceramic brick wall

The annual temperature variations of the indoor air behind the ceramic brick wall for TRY in all studied locations are shown in Fig. 6. For the sake of legibility, only the data for reference plasters are plotted as the differences between indoor temperature distributions for reference and SS-PCM plasters are hard to distinguish on this scale. The details between individual plaster performances are provided further in this section.

The data in Fig. 6 clearly indicates various responses of the constructions to different climatic loads in particular geographical locations. One can see from the results, that some locations require more heating hours, while other locations are typical with more warm days reflecting a more extensive need for cooling. Anyway, the effect of both cooling and heating setpoints is apparent as the data below 20 °C and above 24 °C are trimmed, thus, indicating the heating and cooling regions. The relatively high U -value of uninsulated brick wall has a significant impact on the heat exchange between the conditioned indoor space and the outdoor environment. Since the thermal barrier is missing in the wall assembly, the outdoor climate gains strong impact on the energy efficiency of the PCM plaster applied on the interior surface of the wall. Therefore, warm summers and warm winters represented by Mediterranean climate have positive effects on non-insulated walls with high thermal inertia. The heating and cooling energy consumption summary is given in Table 4. Here, the stress was put on the energy performance improvement by application of different SS-PCM plasters. The analysis was aimed at the identification of the number of heating and cooling hours during the reference year as well as the quantification of energy savings for both heating and cooling. In Table 4, the values of heating, cooling, and total energy are followed by improvements (%) in round brackets for SS-PCM plasters marked as P8, P16, and P24.

The results show only minor improvement to the heating and cooling energy demands after the application of SS-PCM plasters on the interior surface of the ceramic brick wall. The best results were achieved for P24 in Porto, where heating demands were reduced by 3.74% and cooling

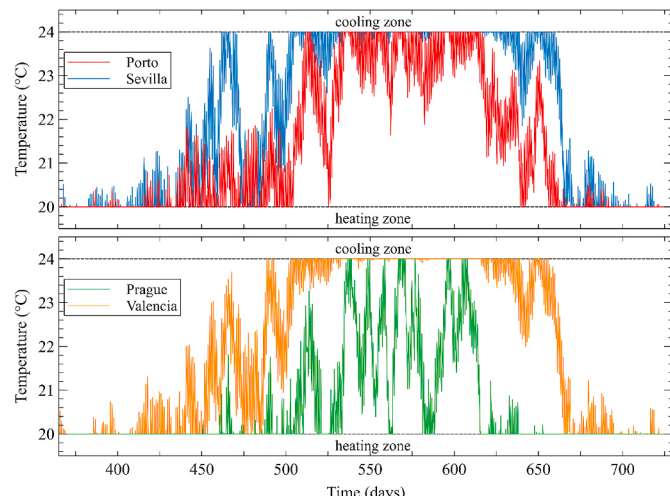


Fig. 6. Indoor air temperature variation during the reference year: ceramic brick wall.

Table 4

Annual space heating and cooling energy analysis per 1 m² of a ceramic brick wall.

		RP	P8	P16	P24
Porto	Heating time (h)	3572	3463	3430	3393
	Heating energy (kWh m ⁻² a ⁻¹)	50.974	49.782 (-2.34%)	49.439 (-3.01%)	49.066 (-3.74%)
	Cooling time (h)	629	620	615	610
	Cooling energy (kWh m ⁻² a ⁻¹)	9.143	8.979 (-1.80%)	8.931 (-2.31%)	8.889 (-2.78%)
	Total energy (kWh m ⁻² a ⁻¹)	60.116	58.760 (-2.26%)	58.731 (-2.90%)	57.995 (-3.60%)
Prague	Heating time (h)	5925	5878	5860	5842
	Heating energy (kWh m ⁻² a ⁻¹)	161.325	160.711 (-0.38%)	160.659 (-0.41%)	160.372 (-0.59%)
	Cooling time (h)	100	95	95	94
	Cooling energy (kWh m ⁻² a ⁻¹)	1.078	1.025 (-4.88%)	1.008 (-6.52%)	0.993 (-7.85%)
	Total energy (kWh m ⁻² a ⁻¹)	162.403	161.737 (-0.41%)	161.667 (-0.45%)	161.365 (-0.64%)
Valencia	Heating time (h)	2680	2637	2623	2603
	Heating energy (kWh m ⁻² a ⁻¹)	39.247	38.660 (-1.49%)	38.510 (-1.88%)	38.332 (-2.33%)
	Cooling time (h)	2490	2479	2476	2476
	Cooling energy (kWh m ⁻² a ⁻¹)	37.353	37.178	37.156	37.118
	Total energy (kWh m ⁻² a ⁻¹)	76.600	75.839 (-0.99%)	75.666 (-1.22%)	75.451 (-1.50%)
Sevilla	Heating time (h)	2556	2508	2489	2468
	Heating energy (kWh m ⁻² a ⁻¹)	35.729	35.008 (-2.02%)	34.802 (-2.59%)	34.591 (-3.18%)
	Cooling time (h)	2655	2643	2640	2637
	Cooling energy (kWh m ⁻² a ⁻¹)	48.276	48.068 (-0.43%)	48.042 (-0.48%)	47.994 (-0.58%)
	Total energy (kWh m ⁻² a ⁻¹)	84.005	83.075 (-1.11%)	82.845 (-1.38%)	82.585 (-1.69%)

demands by 2.78%, generating overall annual savings of approximately 3.60%. Valencia exhibits similar potential for heating energy savings due to Mediterranean winter similar to Porto. However, hot summers in this location are not favorable for this kind of wall assembly. Contrary to those findings, the lowest impact of SS-PCM plaster application was observed for the reference year in Prague, where only 0.64% of total heating and cooling energy was spared. The winter in Prague is too cold, generating no room for PCM to perform phase change transition, and the summer is not hot enough so that air-conditioning is practically useless in this location. However, speaking in absolute values, the savings on heating are ranging from 0.91 to 1.91 kWh·m⁻²·a⁻¹, with the lowest savings identified in Valencia. The savings on cooling were found between 0.09 and 0.28 annually, which is not of great significance. The most beneficial application of SS-PCM plasters was observed for the plaster P24 in Porto, generating annual savings of 2.121 kWh per 1 m² of the façade wall.

4.2. Ceramic brick wall with thermal insulation

The annual temperature variations of the indoor air behind the ceramic brick wall provided with mineral insulation for TRY in all studied locations are shown in Fig. 7. Similarly to Fig. 6, only the data for reference plasters are plotted. Here, the presence of thermal insulation on the exterior side is clearly evident. The thermal insulation reduces heat transfer through the building envelope and enhances the thermal storage of ceramic brick. The effect of thermal barrier imposes significantly higher temperature fluctuations inside the studied room as the heat cannot be simply conducted through the wall like in the previous case.

Contrary to the previous case, where ceramic brick without thermal insulation was analyzed, here, the application of thermal insulation has

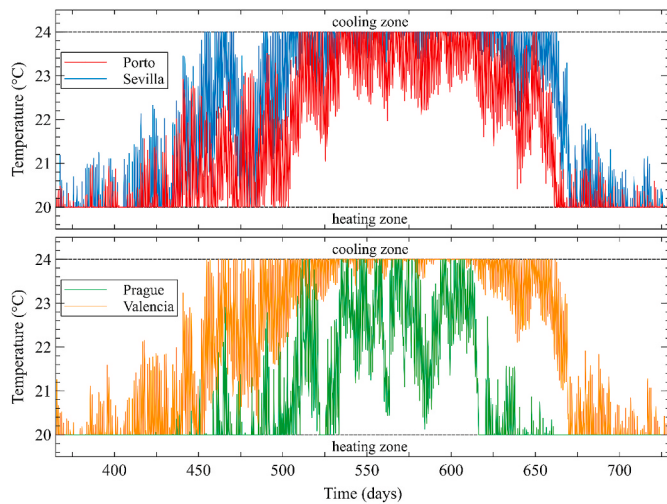


Fig. 7. Indoor air temperature variation during the reference year, ceramic brick wall with thermal insulation.

a beneficial impact on SS-PCM plasters boosting their thermal storage capabilities. Generally speaking, the heat transfer through the opaque building element was reduced, which creates an opportunity for the plasters to store the heat that was accumulated in the interior. Total heating and cooling energy demands were reduced approximately by 30–40% compared to the non-insulated wall. Similarly, the energy savings generated by SS-PCM plasters significantly increased as obvious from Table 5.

The Mediterranean winters with relatively high temperatures create better conditions for generation of heating energy savings contrary to

Table 5
Annual space heating and cooling energy analysis per 1 m² of the ceramic brick wall provided with a thermal insulation layer.

		RP	P8	P16	P24
Porto	Heating time (h)	2739	2646	2615	2568
	Heating energy (kWh m ⁻² a ⁻¹)	27.843	25.947	25.306	24.907
	Cooling time (h)	775	752	746	733
	Cooling energy (kWh m ⁻² a ⁻¹)	10.897	10.486	10.333	10.122
	Total energy (kWh m ⁻² a ⁻¹)	38.740	36.433	35.639	35.029
Prague	Heating time (h)	5384	5316	5288	5268
	Heating energy (kWh m ⁻² a ⁻¹)	96.346	94.777	94.268	93.801
	Cooling time (h)	181	172	167	162
	Cooling energy (kWh m ⁻² a ⁻¹)	1.837	1.690	1.639	1.588
	Total energy (kWh m ⁻² a ⁻¹)	98.183	96.467	95.906	95.389
Valencia	Heating time (h)	2055	1940	1898	1842
	Heating energy (kWh m ⁻² a ⁻¹)	21.573	19.249	18.504	17.940
	Cooling time (h)	2234	2213	2205	2195
	Cooling energy (kWh m ⁻² a ⁻¹)	30.647	30.262	30.145	29.986
	Total energy (kWh m ⁻² a ⁻¹)	52.220	49.511	48.649	47.926
Sevilla	Heating time (h)	1892	1790	1739	1699
	Heating energy (kWh m ⁻² a ⁻¹)	19.145	16.716	15.900	15.354
	Cooling time (h)	2319	2300	2296	2289
	Cooling energy (kWh m ⁻² a ⁻¹)	38.608	38.168	38.049	37.872
	Total energy (kWh m ⁻² a ⁻¹)	57.752	54.884	53.948	53.225

the Continental ones when insulated ceramic brick wall is of interest. Even if the thermal barrier is present, high thermal conductivity of ceramic brick affects the energy storage capability of the interior plaster. Therefore, the performance of the plasters during cold winter in Continental climate region is still very poor. On the other hand, warm summers in Porto, Sevilla and Valencia shifted indoor temperature fluctuations to the range between 23 and 24 °C, which is above the melting point of PCM. Therefore, the potential of cooling energy savings of PCM plasters was not manifested for the current physical setup.

The results indicate significantly higher improvement to the heating and cooling energy demands after the application of SS-PCM plasters on the interior surface of the ceramic brick wall with thermal insulation than in the previous case. The best results were achieved for P24 in Porto, where total annual savings reached approximately 9.56%. However, the other locations of Sevilla and Valencia exhibit significant annual savings as well, 7.84% and 8.22%, respectively. The lowest impact of SS-PCM plaster application was observed for the reference year in Prague, where only 2.85% of total heating and cooling energy was spared. Speaking in absolute values, the savings on heating are ranging from 2.54 to 3.79 kWh·m⁻²·a⁻¹, while savings on cooling show 0.25 to 0.79 kWh·m⁻²·a⁻¹ annually, which is not of great significance. Assuming that cooling is dominant over heating in Sevilla and Valencia, it can be stated that thermal properties of studied PCM in combination with user-defined set points for indoor thermal comfort do not provide enough potential for generation of significant savings on cooling when ceramic brick wall is taken into consideration. The most beneficial application of SS-PCM plasters was observed for the plaster P24 in Sevilla, generating savings of 4.527 kWh·m⁻²·a⁻¹.

4.3. AAC wall

The annual temperature variations of the indoor air behind the AAC wall for TRY in all studied locations are shown in Fig. 8. Similarly to Figs. 6 and 7, only the data for reference plasters are plotted. Here, the substitution of ceramic brick by AAC as a structural material reduced thermal inertia of the load-bearing construction, which brought similar effect as the application of thermal insulation on the ceramic brick wall with one substantial difference, that is a low thermal conductivity and high specific heat capacity of AAC. As a result, the heat was retained inside the building for a longer time, which increased, in combination with the effect of solar heat gains and air infiltration, daily temperature fluctuations. Such conditions proved to be favorable for the application of interior SS-PCM plasters providing them enough room to store the heat that is accumulated during the day inside the building.

At first glance, the thermal performance is very similar to the

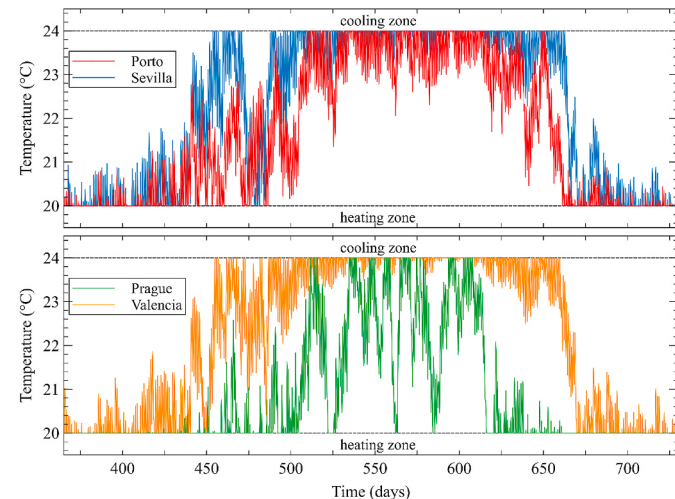


Fig. 8. Indoor air temperature variation during the reference year, AAC wall.

previous case, where insulated ceramic brick wall was analyzed. The number of heating and cooling hours during TRY is very similar to the insulated brick wall since the *U*-value of AAC wall is only slightly lower. However, one important difference should be considered, which is lower thermal conductivity (or thermal inertia) of AAC helping the plasters to store the heat for a longer period. This fact is positively projected in heating and cooling energy consumptions outperforming the case of insulated ceramic brick wall. For a detailed analysis of the energy performance of SS-PCM plasters applied on the AAC wall, please, refer to Table 6.

The results indicate practically identical values for heating energy as those obtained by an insulated ceramic brick wall. However, greater improvements were achieved for cooling energy demands. Therefore, the total energy consumptions are approximately 10–15% lower than in the case of insulated ceramic brick. The considerable savings on heating energy were achieved for the reference years in Valencia and Sevilla, which is caused by warm winters in those regions. The savings on cooling are still not dominant which is caused by melting and solidifying temperature of phase change, which is close to heating setpoint. Although the best results were achieved for P24 in Porto, where total annual savings reached approximately 11.04%, the highest savings in absolute values were observed in Valencia and Sevilla with an annual spare of 4.590 and 4.764 kWh per 1 m² of the façade, respectively. The lowest impact of SS-PCM plaster application was observed for TRY in Prague like in the previous cases, which is caused by cold winters comparing to other studied regions. The annual total energy savings was 3.18% for P24, which is approximately 2.936 kWh·m⁻²·a⁻¹.

4.4. AAC wall with thermal insulation

The annual temperature variations of the indoor air behind the AAC wall with thermal insulation for TRY in all studied locations are shown

Table 6
Annual space heating and cooling energy analysis per 1 m² of AAC wall.

		RP	P8	P16	P24
Porto	Heating time (h)	2521	2424	2391	2359
	Heating energy (kWh m ⁻² a ⁻¹)	25.636	23.557	22.982	22.678
		(-8.11%)	(-10.35%)	(-11.54%)	
	Cooling time (h)	754	726	714	693
	Cooling energy (kWh m ⁻² a ⁻¹)	10.778	10.273	10.058	9.716
		(-4.69%)	(-6.68%)	(-9.85%)	
Prague	Total energy (kWh m ⁻² a ⁻¹)	36.414	33.830	33.041	32.394
		(-7.10%)	(-9.26%)	(-11.04%)	
	Heating time (h)	5230	5161	5146	5128
	Heating energy (kWh m ⁻² a ⁻¹)	90.152	88.545	88.044	87.679
		(-1.78%)	(-2.34%)	(-2.74%)	
	Cooling time (h)	212	197	194	184
Valencia	Cooling energy (kWh m ⁻² a ⁻¹)	2.319	2.069	1.980	1.856
		(-10.77%)	(-14.64%)	(-19.98%)	
	Total energy (kWh m ⁻² a ⁻¹)	92.471	90.615	90.024	89.535
		(-2.01%)	(-2.65%)	(-3.18%)	
	Heating time (h)	1854	1737	1705	1650
	Heating energy (kWh m ⁻² a ⁻¹)	19.924	17.436	16.795	16.290
Sevilla		(-12.49%)	(-15.71%)	(-18.24%)	
	Cooling time (h)	2142	2114	2103	2089
	Cooling energy (kWh m ⁻² a ⁻¹)	29.836	29.283	29.125	28.880
		(-1.85%)	(-2.38%)	(-3.20%)	
	Total energy (kWh m ⁻² a ⁻¹)	49.760	46.719	45.920	45.170
		(-6.11%)	(-7.72%)	(-9.22%)	
Sevilla	Heating time (h)	1704	1583	1543	1501
	Heating energy (kWh m ⁻² a ⁻¹)	17.593	15.055	14.389	13.912
		(-14.42%)	(-18.21%)	(-20.93%)	
	Cooling time (h)	2248	2226	2223	2213
	Cooling energy (kWh m ⁻² a ⁻¹)	37.542	36.908	36.733	36.459
		(-1.69%)	(-2.15%)	(-2.88%)	
	Total energy (kWh m ⁻² a ⁻¹)	55.135	51.963	51.122	50.371
		(-5.75%)	(-7.28%)	(-8.64%)	

in Fig. 9. Similarly to Figs. 6–8, only the data for reference plasters are plotted. The results show that the AAC wall with thermal insulation exhibited the highest diurnal temperatures of the indoor air. The highest thermal resistance of this wall assembly induced highest temperature fluctuations of the interior surpassing phase change temperature repeatedly during the reference year, thus providing the most favorable conditions of the SS-PCM plasters to prove their latent heat storage capabilities among all studied assemblies.

Thermal performances of the SS-PCM plasters are summarized in Table 7 in detail. When compared to the previous wall assemblies, the insulated AAC wall achieved the best results regarding the SS-PCM plasters. Similarly to the previous cases, the melting and solidification temperature that is closer to heating than cooling setpoint in the studied room turned the major part of savings to those related with heating. This is valid also for regions of Valencia and Sevilla where cooling is dominant over heating during the year.

Similar to previous cases, the best performance of SS-PCM plasters was observed for the reference years in Porto, Valencia, and Sevilla, where the savings ranged between 13 and 16%. The highest reduction of heating energy was registered in Sevilla with 29.20%. In the same manner, the best achievement in cooling energy reduction was observed for Prague with 23.16%. However, from a practical point of view, the biggest cooling energy savings in absolute values of 1.647 and 1.734 kWh·m⁻²·a⁻¹ were identified in Porto and Sevilla, respectively. The annual heating energy savings of 4.660 and 4.812 kWh·m⁻²·a⁻¹ for P24 plaster in Valencia and Sevilla, respectively, are the highest registered improvements among the studied assemblies and locations. The highest reduction of total heating and cooling energy was observed in Sevilla, where approximately 6.546 kWh per square meter of the façade could be spared annually after the application of P24 plaster on the interior surface.

5. Discussion

The thermal performance of building envelopes represents a very attractive topic with significant importance since the environmental goals require dramatic energy consumption decrease. The significant influence of PCMs on the possible energy savings was proved by many studies reflected by high numbers of published papers in the Web of Science.

5.1. Interpretation of the results

Generally, the application of PCMs in building envelope

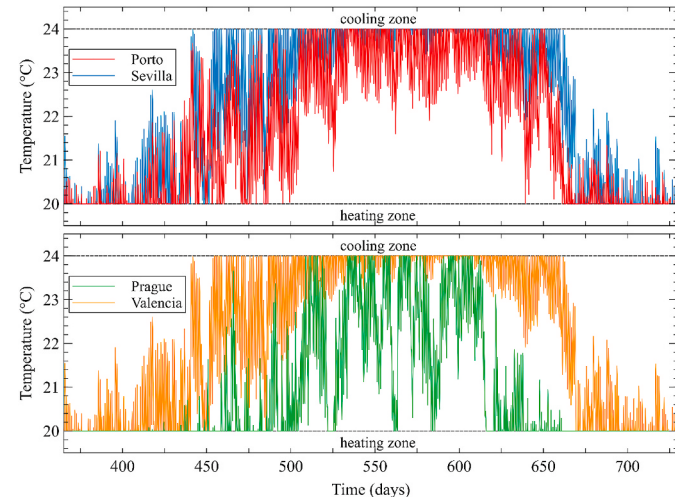


Fig. 9. Indoor air temperature variation during the reference year: AAC wall with thermal insulation.

Table 7

Annual space heating and cooling energy analysis per 1 m² of AAC wall with a thermal insulation layer.

		RP	P8	P16	P24
Porto	Heating time (h)	2498	2400	2360	2308
	Heating energy (kWh m ⁻² a ⁻¹)	24.115	21.368	20.589	19.938
			(-11.39%)	(-14.62%)	(-17.32%)
	Cooling time (h)	843	802	792	764
	Cooling energy (kWh m ⁻² a ⁻¹)	11.877	11.042	10.713	10.230
			(-7.04%)	(-9.80%)	(-13.87%)
Prague	Total energy (kWh m ⁻² a ⁻¹)	35.993	32.409	31.303	30.169
			(-9.96%)	(-13.03%)	(-16.18%)
	Heating time (h)	5220	5141	5120	5073
	Heating energy (kWh m ⁻² a ⁻¹)	85.056	83.010	82.366	81.700
			(-7.92%)	(-8.64%)	(-9.37%)
	Cooling time (h)	279	243	234	213
Valencia	Cooling energy (kWh m ⁻² a ⁻¹)	2.955	2.583	2.447	2.270
			(-12.60%)	(-17.19%)	(-23.16%)
	Total energy (kWh m ⁻² a ⁻¹)	88.011	85.592	84.813	83.971
			(-2.75%)	(-3.63%)	(-4.59%)
	Heating time (h)	1842	1718	1684	1620
	Heating energy (kWh m ⁻² a ⁻¹)	18.734	15.700	14.935	14.074
Sevilla			(-16.20%)	(-20.28%)	(-24.88%)
	Cooling time (h)	2168	2133	2120	2096
	Cooling energy (kWh m ⁻² a ⁻¹)	30.152	29.318	29.028	28.620
			(-2.77%)	(-3.73%)	(-5.08%)
	Total energy (kWh m ⁻² a ⁻¹)	48.886	45.018	43.963	42.694
			(-9.53%)	(-11.65%)	(-14.20%)
Sevilla	Heating time (h)	1684	1577	1533	1474
	Heating energy (kWh m ⁻² a ⁻¹)	16.481	13.417	12.661	11.669
			(-18.59%)	(-23.18%)	(-29.20%)
	Cooling time (h)	2260	2236	2225	2209
	Cooling energy (kWh m ⁻² a ⁻¹)	37.505	36.560	36.236	35.771
			(-2.52%)	(-3.38%)	(-4.62%)
Total energy (kWh m ⁻² a ⁻¹)	53.986	49.977	48.897	47.440	
			(-9.35%)	(-11.31%)	(-13.96%)

compositions reduce space heating and cooling in certain periods while preserving thermal comfort of the occupants. However, the way the results are presented is crucial for understanding the benefits of PCMs under real conditions. In other words, the achieved results need to be analyzed on a comparable scale since the percentual interpretation does not provide an immediate information required by investors and stakeholders [78–80]. To assess the relevant benefits, the absolute savings in kWh represent a more appropriate form of presentation, expressing the economic viability of PCMs applied in conventional building materials. For example, Parameshwaran and Kalaiselvam [82] reported savings of silver nano-based PCM in the range of 7.5–50%, which might sound very promising. However, advanced systems of heat recuperation, storage and distribution were used, which devalued the real benefit of that application. A much better and closer comparison of PCMs benefits for potential energy savings can be found in the study published by Biswas et al. [83], where the annual heat gains for different wallboards and orientations were investigated. The annual vs. peak summer behavior of the PCM wallboard was dictated by the interior cooling set point relative to the phase change temperature range of the PCMs. In summary, the average heat gains due to the incorporated PCM amounted from 7.04 to 20.73% according to the orientation of the wall. Nonetheless, those numbers as well as in several other studies access only percentual improvements often related only to specific days or season.

As the outputs of this case study are presented in both absolute and percentual values, it can be used to show the importance of proper interpretation as some numbers in a percentual presentation may look very promising, the real benefit is practically negligible though. Such data can be found in the case of insulated and non-insulated AAC walls in Prague, where the savings of cooling energy were reported as 19.98 and 23.16%, respectively (see Tables 6 and 7). The real savings

expressed in absolute values revealed only 0.463 and 0.685 kWh per square meter of the wall annually, which should not be considered as a valuable benefit at all. Therefore, the absolute values of energy savings or space heating or cooling demands related to the square meter of façade wall of floor area are very important to understand the real benefit of PCMs application. Such data can be subsequently used for the assessment of suitability and economic feasibility of PCM applications for particular construction in particular location.

5.2. Effect of climatic load and wall composition

As described in several studies [6,13,36], the location of building equipped by PCM elements need to be considered for optimal and efficient design of heating/cooling solutions. Apart from the cooling demands which are typical for hot regions, the energy savings related to colder regions pose another task for PCMs adjustments. In other words, the experimental studies aimed at the investigation of PCM suitability must be linked with a detail climate characterization in order to provide a useful tool for PCM utilization design. For the ideal function of the plaster improved by SS-PCM admixture, bigger temperature differences between day and night are required to complete the phase transition of SS-PCM.

While many research papers [64,84–86] contemplate about the influence of PCM thickness, encapsulation technique, melting temperature, climatic conditions, the effect of load-bearing material and applied PCMs is studied rarely even though PCMs were proposed as an efficient tool mainly for light-weighted building envelopes which have reduced temperature peak resistance. Apparently, the effect of incorporated PCMs into concrete [87–89] is diminished compared to other materials such as wallboards or plasters applied on load-bearing materials with low thermal inertia.

The result presented in this paper demonstrate how the location and material composition influence the energy and thermal performance of applied SS-PCM plasters. There exist two dependencies that can be clearly observed from the results presented in this research. First, the effectiveness of PCM applications increases with increasing average outdoor temperature, i.e. the regions with higher outdoor temperature proved to be more suitable for application of PCM plasters with phase change transition zone close to the human comfort room temperatures. Second, the application of PCM is more efficient when low thermal transmittance (*U*-value) or thermal inertia of building envelope is assured. Of course, the *U*-value is not the only parameter influencing the effectiveness of that application, as there exist several other factors influencing the performance, such as sequence of materials in wall composition, specific heat capacity and thermal conductivity of materials involved in the wall assembly, glazing percentage, ventilation rate, etc. However, the *U*-value of the wall assembly as commonly accepted parameter can be simply used as some general correlation is apparent from the data presented in Tables 4–7. Moreover, if both correlations are combined together, a simple and trivial relation can be introduced for a rapid assessment of suitability and energy efficiency of PCM applications. The correlation between location, wall assembly and efficiency of PCM applications is shown in Fig. 10. Here, the X-axis is represented by annual average temperature in particular location divided by *U*-value of respective wall assembly, while Y-axis shows the absolute annual savings per square meter of façade.

In the light of the findings shown above, the continental climate, represented by Prague, proved to be the least suitable for the application of SS-PCM plasters investigated in this research. Although the plasters generated savings in any application in this study, the annual spare between 1.038 and 4.040 kWh·m⁻² brought a rather unpromising perspective indicating that PCM with different phase change temperatures should be of interest for Prague-like locations. The only result from the continental climate zone that could be partially accepted comes from the insulated AAC wall revealing that only wall assemblies with high thermal resistance should be considered for the application of P24

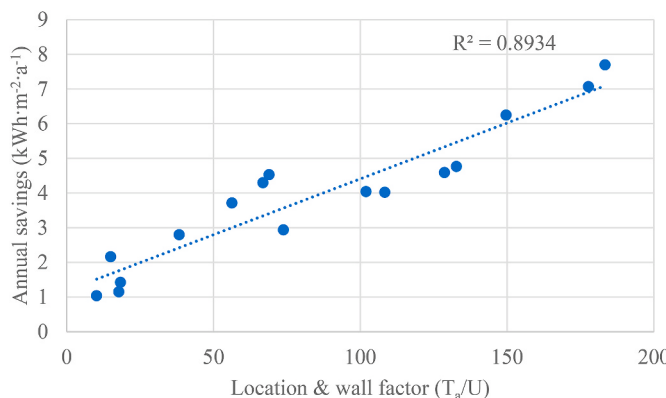


Fig. 10. Correlation of the effectiveness of PCM application with climatic load and wall assembly.

plasters.

More promising results were observed for dry and temperate climates with hot and warm summers, with the annual savings between 3.711 and 6.546 kWh per square meter of the façade for wall assemblies with improved thermal resistance. Therefore the uninsulated brick wall was excluded from the above range. Assuming that the total area of façade walls in common apartments may range from 15 to 100 m² depending on the apartment size and layout, the total savings may range from approximately 55 to 650 kWh per year. In any case, the economic feasibility of PCM plaster application is not unambiguous, considering the cost of PCM agents and payback period given by current energy prices and costs. However, environmental benefits may counterbalance the economical drawbacks in some regions if the application of PCM is planned carefully.

6. Conclusions

A computational analysis of energy performance of an interior plaster modified using 8, 16, and 24 wt% of SS-PCM based on diatomite and *n*-dodecanol was performed. A particular attention was paid to the effects of temperature, material performance during the winter/summer periods, thermal insulation, construction materials, and energy consumption in four locations across the EU.

The calculated heat transmission showed a slight positive effect of SS-PCM layer on the interior climate and manifested its ability to reduce heat flux densities during the peak periods. The heat transmission from/to the interior decreased with the increasing amount of SS-PCM incorporated in the plaster which resulted in annual energy savings on heating and cooling. Although the positive effect of SS-PCM integrated in plaster mixtures was clearly demonstrated, the energy performance proved to be very sensitive to climatic loads and material composition of wall assembly. Therefore, the application of SS-PCM plasters in certain locations or wall assemblies was found unsuitable from both economic and environmental points of view.

The obtained results provided important data and practical guidelines regarding the utilization of latent heat storage systems in residential buildings in Europe with respect to various climatic loads and material compositions. The following outputs can be highlighted:

- PCM containing plasters cannot be considered as an effective energy saving measure in the building sector in general. Each wall assembly must be carefully considered with respect to the climatic load to maximize the energy saving potential of a particular latent heat storage layer.
- The energy saving potential of PCM plasters increases with decreasing *U*-value. Therefore, building envelopes with load-bearing materials having low thermal conductivity or thermally insulated

wall assemblies can be considered as the most suitable for using a latent heat storage layer on the interior side.

- The continental climate excludes the application of a PCM plaster as an efficient energy-saving measure in building envelopes.
- There exists a strong correlation between thermal transmittance of building envelope, climatic load and energy saving potential, which can be used for an initial estimation of the energy efficiency of PCM integration into a wall assembly.
- A proper interpretation of computational results is of high importance as some numbers in a percentual presentation may look very promising but the real benefit is practically negligible.
- Considering the size and layout of common apartments built in Europe, the application of SS-PCM plasters on the interior surface of building envelopes may generate annual savings between 55 and 650 kWh in precisely tailored applications. However, a general view of using PCM plasters as an effective tool for reduction of heating and cooling energy demands is not unambiguous.

CRediT author statement

Jan Kočí: Methodology, Software, Formal analysis, Funding acquisition, Writing - Original Draft Jan Fořt: Conceptualization, Methodology, Investigation, Visualisation, Writing - Original Draft Robert Černý: Writing - Review & Editing, Supervision, Project administration.

Declaration of competing interest

The authors declare that they have no known competing financial interests or personal relationships that could have appeared to influence the work reported in this paper.

Acknowledgment

This research has been supported by the Czech Science Foundation, under project No 20-01504S.

References

- [1] IEA. Paris, France: Energy End-Use: Buildings; 2018.
- [2] Sain Akadiri S, Alola AA, Olaschinde-Williams G, Etokakpan MU. The role of electricity consumption, globalization and economic growth in carbon dioxide emissions and its implications for environmental sustainability targets. Sci Total Environ 2020;708:10.
- [3] Jeon J, Lee J, Ham Y. Quantifying the impact of building envelope condition on energy use. Build Res Inf 2019;47(4):404–20.
- [4] Ma MD, Cai WG, Wu Y. China act on the energy efficiency of civil buildings (2008): a decade review. Sci Total Environ 2019;651:42–60.
- [5] McArthur JJ, Powell C. Health and wellness in commercial buildings: systematic review of sustainable building rating systems and alignment with contemporary research. Build Environ 2020;171:18.
- [6] Solgi E, Hamedani Z, Fernando R, Kari BM, Skates H. A parametric study of phase change material behaviour when used with night ventilation in different climatic zones. Build Environ 2019;147:327–36.
- [7] Zuhail S, Manton R, Griffin C, Hajdukiewicz M, Keane MM, Goggins J. An Indoor Environmental Quality (IEQ) assessment of a partially-retrofitted university building. Build Environ 2018;139:69–85.
- [8] Fort J, Beran P, Pavlik Z, Černý R. Complex assessment of reconstruction works on an institutional building: a case study. J Clean Prod 2018;202:871–82.
- [9] Memon SA. Phase change materials integrated in building walls: a state of the art review. Renew Sustain Energy Rev 2014;31:870–906.
- [10] Tyagi VV, Buddhi D. PCM thermal storage in buildings: a state of art. Renewable & Renew Sust Energ Rev 2007;11(6):1146–66.
- [11] Rathore PKS, Shukla SK, Gupta NK. Potential of microencapsulated PCM for energy savings in buildings: a critical review. Sustain Cities Soc 2020;53:21.
- [12] Mofijur M, Mahlia TMI, Silitonga AS, Ong HC, Silakhorri M, Hasan MH, et al. Phase change materials (PCM) for solar energy usages and storage: an overview. Energies 2019;12(16):20.
- [13] Bhambhani DK, Rathod MK, Banerjee J. Passive cooling techniques for building and their applicability in different climatic zones-The state of art. Energy Build 2019; 198:467–90.
- [14] Oropeza-Perez I, Ostergaard PA. Active and passive cooling methods for dwellings: a review. Renew Sustain Energy Rev 2018;82:531–44.

- [15] Guardia C, Schicchi DS, Caggiano A, Barluenga G, Koenders E. On the capillary water absorption of cement-lime mortars containing phase change materials: experiments and simulations. *Build Simul-China* 2020;13(1):19–31.
- [16] Song MJ, Niu FX, Mao N, Hu YX, Deng SM. Review on building energy performance improvement using phase change materials. *Energy Build* 2018;158:776–93.
- [17] Madad A, Mouhib T, Mouhsen A. Phase change materials for building applications: a thorough review and new perspectives. *Buildings* 2018;8:63.
- [18] Sarcinella A, De Aguiar JLB, Lettieri M, Cunha S, Frigione M. Thermal performance of mortars based on different binders and containing a novel sustainable phase change material (PCM). *Materials* 2020;13:2055.
- [19] Bao XH, Yang HB, Xu XX, Xu T, Cui HZ, Tang WC. Development of a stable inorganic phase change material for thermal energy storage in buildings. *Sol Energy Mater Sol Cells* 2020;208:110420.
- [20] Zhang Y, Liu H, Niu JF, Wang XD, Wu DZ. Development of reversible and durable thermochromic phase-change microcapsules for real-time indication of thermal energy storage and management. *Appl Energy* 2020;264:114729.
- [21] Joseph A, Kabbara M, Groulx D, Allred P, White MA. Characterization and real-time testing of phase-change materials for solar thermal energy storage. *Int J Energy Res* 2016;40(1):61–70.
- [22] Cheng JJ, Zhou Y, Ma D, Li SX, Zhang F, Guan Y, Qu WJ, Jin Y, Wang D. Preparation and characterization of carbon nanotube microcapsule phase change materials for improving thermal comfort level of buildings. *Construct Build Mater* 2020;244:118388.
- [23] Han DM, Lougou BG, Xu YT, Shuai Y, Huang X. Thermal properties characterization of chloride salts/nanoparticles composite phase change material for high-temperature thermal energy storage. *Appl Energy* 2020;264:114674.
- [24] Essid N, Loulizi A, Neji J. Compressive strength and hygric properties of concretes incorporating microencapsulated phase change material. *Construct Build Mater* 2019;222:254–62.
- [25] Fort J, Novotny R, Trník A, Černý R. Preparation and characterization of novel plaster with improved thermal energy storage performance. *Energies* 2019;12(17):13.
- [26] Li CE, Yu H, Song Y. Experimental investigation of thermal performance of microencapsulated PCM-contained wallboard by two measurement modes. *Energy Build* 2019;184:34–43.
- [27] Olivieri L, Tenorio JA, Revuelta D, Navarro L, Cabeza LF. Developing a PCM-enhanced mortar for thermally active precast walls. *Construct Build Mater* 2018;181:638–49.
- [28] Souayfane F, Fardoun F, Biwole PH. Phase change materials (PCM) for cooling applications in buildings: a review. *Energy Build* 2016;129:396–431.
- [29] Sirmelis R, Vanaga R, Freimanis R, Blumberga A. Solar facade module for nearly zero energy building. Optimization strategies. *Environ Clim Technol* 2019;23:170–81.
- [30] Lagou A, Kyliki A, Sadauskienė J, Fokaides PA. Numerical investigation of phase change materials (PCM) optimal melting properties and position in building elements under diverse conditions. *Construct Build Mater* 2019;225:452–64.
- [31] Figueiredo A, Vicente R, Lapa J, Cardoso C, Rodrigues F, Kampf J. Indoor thermal comfort assessment using different constructive solutions incorporating PCM. *Appl Energy* 2017;208:1208–21.
- [32] Fateh A, Borelli D, Weinlaender H, Devia F. Cardinal orientation and melting temperature effects for PCM-enhanced light-walls in different climates. *Sustain Cities Soc* 2019;51:19.
- [33] Johra H, Heiselberg P, Le Dreau J. Influence of envelope, structural thermal mass and indoor content on the building heating energy flexibility. *Energy Build* 2019;183:325–39.
- [34] Park JH, Jeon J, Lee J, Wi S, Yun BY, Kim S. Comparative analysis of the PCM application according to the building type as retrofit system. *Build Environ* 2019;151:291–302.
- [35] Ahangari M, Maerefat M. An innovative PCM system for thermal comfort improvement and energy demand reduction in building under different climate conditions. *Sustain Cities Soc* 2019;44:120–9.
- [36] Kim HB, Mae M, Choi Y. Application of shape-stabilized phase-change material sheets as thermal energy storage to reduce heating load in Japanese climate. *Build Environ* 2017;125:1–14.
- [37] Alam M, Jamil H, Sanjayan J, Wilson J. Energy saving potential of phase change materials in major Australian cities. *Energy Build* 2014;78:192–201.
- [38] Aranda-Uson A, Ferreira G, López-Sabirón AM, Mainar-Toledo MD, Zabalza Bribián I. Phase change material applications in buildings: an environmental assessment for some Spanish climate severities. *Sci Total Environ* 2013;444:16–25.
- [39] Kharbouch Y, Mimet A, El Ganaoui M, Ouhsaine L. Thermal energy and economic analysis of a PCM-enhanced household envelope considering different climatic zones in Morocco. *Int J Sustain Energy* 2018;37:515–32.
- [40] Aketouane Z, Malha M, Bruneau D, Bah A, Michel B, Asbik M, Ansari O. Energy savings potential by integrating Phase Change Material into hollow bricks: the case of Moroccan buildings. *Build Simul-China* 2018;11:1109–22.
- [41] Saxena R, Agarwal N, Rakshit D, Kaushik SC. Suitability assessment and experimental characterization of phase change materials for energy conservation in Indian buildings. *J Sol Energ-T ASME* 2020;142:011014.
- [42] Hasan A, Al-Sallal KA, Rashid Y, Abdelbaqi S. Effect of phase change materials (PCMs) integrated into a concrete block on heat gain prevention in a hot climate. *Sustainability-Basel* 2016;8:1009.
- [43] Ahangari M, Maerefat M. An innovative PCM system for thermal comfort improvement and energy demand reduction in building under different climate conditions. *Sustain Cities Soc* 2019;44:120–9.
- [44] Park JH, Wi S, Chang SJ, Kim S. Analysis of energy retrofit system using latent heat storage materials applied to residential buildings considering climate. *Impacts* 2020;169:114904.
- [45] Sovetova M, Memon SA, Kim J. Thermal performance and energy efficiency of building integrated with PCMs in hot desert climate region. *Sol Energy* 2019;189:357–71.
- [46] Lei J, Yang J, Yang EH. Energy performance of building envelopes integrated with phase change materials for cooling load reduction in tropical Singapore. *Appl Energy* 2016;162:207–17.
- [47] Panchabikesan K, Joybari MM, Haghigat F, Ramalingam V, Ding Y. Feasibility study on the year-round operation of PCM based free cooling systems in tropical climatic conditions. *Energy* 2020;192:116695.
- [48] Kenzhekanov S, Memon SA, Adilkhanova I. Quantitative evaluation of thermal performance and energy saving potential of the building integrated with PCM in a subarctic climate. *Energy* 2020;192:116607.
- [49] Jangeldinov B, Memon SA, Kim J, Kabdrakhanova M. Evaluating the energy efficiency of PCM-integrated lightweight steel-framed building in eight different cities of warm summer humid continental climate. *Ann Mater Sci Eng* 2020;2020:4381495.
- [50] Costanzo V, Evola G, Marletta L, Nocera F. The effectiveness of phase change materials in relation to summer thermal comfort in air-conditioned office buildings. *Build Simul-China* 2018;11(6):1145–61.
- [51] Solgi E, Hamedani Z, Fernando R, Kari BM. A parametric study of phase change material characteristics when coupled with thermal insulation for different Australian climatic zones. *Build Environ* 2019;163:8.
- [52] Firlag S, Zawada B. Impacts of airflows, internal heat and moisture gains on accuracy of modeling energy consumption and indoor parameters in passive building. *Energy Build* 2013;64:372–83.
- [53] Lachheb M, Younsi Z, Hassane N, Karkri M, Ben Nasrallah S. Thermal behavior of a hybrid PCM/plaster: a numerical and experimental investigation. *Appl Therm Eng* 2017;111:49–59.
- [54] Soudian S, Berardi U. Assessing the effect of night ventilation on PCM performance in high-rise residential buildings. *J Build Phys* 2019;43:229–49.
- [55] Pominowski M, Heiselberg P, Jensen RL. Full-scale investigation of the dynamic heat storage of concrete decks with PCM and enhanced heat transfer surface area. *Energy Build* 2013;59:287–300.
- [56] Kusama Y, Ishidoya Y. Thermal effects of a novel phase change material (PCM) plaster under different insulation and heating scenarios. *Energy Build* 2017;141:226–37.
- [57] Strifith U, Tyagi VV, Stropnik R, Paksoy H, Haghigat F, Joybari MM. Integration of passive PCM technologies for net-zero energy buildings. *Sustain Cities Soc* 2018;41:286–95.
- [58] Bruno F, Tay NHS, Belusko M. Minimising energy usage for domestic cooling with off-peak PCM storage. *Energy Build* 2014;76:347–53.
- [59] Aketouane Z, Malha M, Bruneau D, Bah A, Michel B, Asbik M, et al. Energy savings potential by integrating Phase Change Material into hollow bricks: the case of Moroccan buildings. *Build Simul-China* 2018;11(6):1109–22.
- [60] Mehling H, Barreneche C, Sole A, Cabeza LF. The connection between the heat storage capability of PCM as a material property and their performance in real scale applications. *J Energ Stor* 2017;13:35–9.
- [61] Barz T, Sommer A. Modeling hysteresis in the phase transition of industrial-grade solid/liquid PCM for thermal energy storages. *Int J Heat Mass Tran* 2018;127:701–13.
- [62] Bahrar M, Djamel ZI, El Mankibi M, Larbi AS, Salvia M. Numerical and experimental study on the use of microencapsulated phase change materials (PCMs) in textile reinforced concrete panels for energy storage. *Sustain Cities Soc* 2018;41:455–68.
- [63] Qiao YH, Yang L, Bao JY, Liu Y, Liu JP. Reduced-scale experiments on the thermal performance of phase change material wallboard in different climate conditions. *Build Environ* 2019;160:12.
- [64] Park JH, Lee J, Wi S, Jeon J, Chang SJ, Chang JD, et al. Optimization of phase change materials to improve energy performance within thermal comfort range in the South Korean climate. *Energy Build* 2019;185:12–25.
- [65] AlParís F, Juádiz A, Manzano-Agugliaro F. Energy retrofit strategies for housing sector in the arid climate. *Energy Build* 2016;131:158–71.
- [66] Zeinelabdein R, Ömer S, Gan GH. Experimental performance of latent thermal energy storage for sustainable cooling of buildings in hot-arid regions. *Energy Build* 2019;186:169–85.
- [67] Sinka M, Bajare D, Jakovics A, Ratnies J, Gendelis S, Tihana J. Experimental testing of phase change materials in a warm-summer humid continental climate. *Energy Build* 2019;195:205–15.
- [68] Curpek J, Čekon M. Climate response of a BiPV facade system enhanced with latent PCM-based thermal energy storage. *Renew Energy* 2020;152:368–84.
- [69] Markarian E, Fazelour B. Multi-objective optimization of energy performance of a building considering different configurations and types of PCM. *Sol Energy* 2019;191:481–96.
- [70] Fort J, Trník A, Pavlikova M, Pavlik Z, Černý R. Fabrication of dodecanol/diatomite shape-stabilized PCM and its utilization in interior plaster. *Int J Thermophys* 2018;39(12):11.
- [71] Jerman M, Keppert M, Vyborny J, Černý R. Hygric, thermal and durability properties of autoclaved aerated concrete. *Construct Build Mater* 2013;41:352–9.
- [72] Madera J, Koci V, Koci J, Černý R. Physical and mathematical models of hydrothermal processes in historical building envelopes. In: Simos TE, Kalogiratou Z, Monovasilis T, editors. Proceedings of the international conference of computational methods in sciences and engineering 2017; 2017.

- [74] Madera J, Koci J, Koci V, Kruis J. Parallel modeling of hygrothermal performance of external wall made of highly perforated bricks. *Adv Eng Software* 2017;113: 47–53.
- [75] Lewis RW, Ravindren K. Finite element simulation of metal casting. *Int J Numer Methods Eng* 2000;47(1–3):29–59.
- [76] Kruis J, Koudelka T, Krejci T. Efficient computer implementation of coupled hydro-thermo-mechanical analysis. *Math Comput Simulat* 2010;80(8):1578–88.
- [77] Koci J, Madera J, Jerman M, Dolezelova M, Cerny R, IOP. Computational simulation of hygrothermal processes in historical building envelopes provided with interior thermal insulation. In: Florence heri-tech - the future of heritage science and technologies; 2018.
- [78] Peel MC, Finlayson BL, McMahon TA. Updated world map of the Koppen-Geiger climate classification. *Hydrol Earth Syst Sci* 2007;11(5):1633–44.
- [79] Mi XM, Liu R, Cui HZ, Memon SA, Xing F, Lo Y. Energy and economic analysis of building integrated with PCM in different cities of China. *Appl Energy* 2016;175: 324–36.
- [80] Solgi E, Memarian S, Moud GN. Financial viability of PCMs in countries with low energy cost: a case study of different climates in Iran. *Energy Build* 2018;173: 128–37.
- [82] Parameshwaran R, Kalaiselvam S. Energy conservative air conditioning system using silver nano-based PCM thermal storage for modern buildings. *Energy Build* 2014;69:202–12.
- [83] Biswas K, Lu J, Soroushian P, Shrestha S. Combined experimental and numerical evaluation of a prototype nano-PCM enhanced wallboard. *Appl Energy* 2014;131: 517–29.
- [84] Jeong SG, Wi S, Chang SJ, Lee J, Kim S. An experimental study on applying organic PCMs to gypsum-cement board for improving thermal performance of buildings in different climates. *Energy Build* 2019;190:183–94.
- [85] Ye RD, Zhang C, Sun WC, Fang XM, Zhang ZG. Novel wall panels containing CaCl₂ center dot 6H₂O-Mg(NO₃)₂center dot 6H₂O/expanded graphite composites with different phase change temperatures for building energy savings. *Energy Build* 2018;176:407–17.
- [86] Zhu N, Li SS, Hu PF, Wei S, Deng RJ, Lei F. A review on applications of shape-stabilized phase change materials embedded in building enclosure in recent ten years. *Sustain Cities Soc* 2018;43:251–64.
- [87] Entrop AG, Brouwers HJH, Reinders A. Experimental research on the use of micro-encapsulated Phase Change Materials to store solar energy in concrete floors and to save energy in Dutch houses. *Sol Energy* 2011;85(5):1007–20.
- [88] Erlbeck L, Schreiner P, Schlachter K, Dornhofer P, Fasel F, Methner FJ, et al. Adjustment of thermal behavior by changing the shape of PCM inclusions in concrete blocks. *Energy Convers Manag* 2018;158:256–65.
- [89] Xu BW, Li ZJ. Paraffin/diatomite composite phase change material incorporated cement-based composite for thermal energy storage. *Appl Energy* 2013;105: 229–37.